fermentation

MDPI

Article

Monascus purpureus Fermented Product Ameliorates Learning and Memory Impairment in the Amyloid Precursor Protein Transgenic J20 Mouse Model of Alzheimer's Disease

Ming-Chih Fang [1,2], Irene Han-Juo Cheng [3,†] and Chien-Li Chen [1,2,*,†]

[1] Department of Food Science, National Taiwan Ocean University, No. 2, Beining Rd., Zhongzheng Dist., Keelung 20224, Taiwan; mcfang@mail.ntou.edu.tw
[2] Center of Excellence for the Oceans, National Taiwan Ocean University, No. 2, Beining Rd., Zhongzheng Dist., Keelung 20224, Taiwan
[3] Institute of Brain Science, National Yang-Ming University, Taipei 11221, Taiwan; hjcheng@ym.edu.tw
* Correspondence: sander.chen@mail.ntou.edu.tw; Tel.: +886-2-2462-2192 (ext. 5131); Fax: +886-2-2463-4203
† These authors contributed equally to this work.

Abstract: Evidence suggests that various hallmarks such as amyloid overproduction, tau dysfunction, insulin resistance/diabetic mechanisms, and neuroinflammation are associated with Alzheimer's disease (AD). This study investigated the bioactive functions of ankaflavin (AK) and monascin (MS) in the fermented product of *Monascus purpureus* and found their abilities to ameliorate AD by modifying several important pathogenic factors including improved cognitive function, reversed behavioral deficits, reduced hippocampal β-amyloid peptide (Aβ) burden, decreased tau hyper-phosphorylation, and reduced neuroinflammation in the J20 mouse model of AD compared to wild type. *Monascus purpureus* fermented product (MPFP) was suggested to act as a peroxisome proliferator-activated receptor (PPAR)-γ agonist and it was compared against the action of a well-known anti-diabetic PPAR-γ agonist rosiglitazone. MPFP could be a promising therapeutic strategy for disease modification in AD.

Keywords: Alzheimer's disease; transgenic J20 mice; *Monascus purpureus* fermented product; monascin; ankaflavin; peroxisome proliferator-activated receptor-γ

Citation: Fang, M.-C.; Cheng, I.H.-J.; Chen, C.-L. *Monascus purpureus* Fermented Product Ameliorates Learning and Memory Impairment in the Amyloid Precursor Protein Transgenic J20 Mouse Model of Alzheimer's Disease. *Fermentation* **2022**, *8*, 193. https://doi.org/10.3390/fermentation8050193

Academic Editor: Hiroshi Kitagaki

Received: 10 March 2022
Accepted: 20 April 2022
Published: 24 April 2022

1. Introduction

Alzheimer's disease (AD), the most common neurodegenerative dementia worldwide, is characterized by progressive memory and cognitive decline accompanied by functional and behavioral deficits. AD is neuropathologically characterized by neocortical amyloid neuritic plaques containing β-amyloid (Aβ), neurofibrillary tangles (NFT) composed of hyper-phosphorylated tau protein, and widespread synaptic and neuronal loss. Brain Aβ is generated by the coordinated cleavage of the amyloid precursor protein (APP) by β-secretase (BACE1) and γ-secretase [1], and both monomeric and aggregated forms of Aβ may be neurotoxic [2]. Consequently, Aβ-mediated release of pro-inflammatory cytokines, including interleukin (IL)-1β, IL-6, and tumor necrosis factor (TNF)-α, by brain microglia and astrocytes, may contribute to synaptic and neuronal demise [3]. Perhaps related to Aβ toxicity, abnormal tau hyperphosphorylation leads to intracellular aggregated paired helical filaments and NFTs, as well as microtubular instability, and axonal transport defects [1].

Recently, type 2 diabetes mellitus (T2DM) has been shown to increase the risk of dementia, AD, and functional resistance to insulin receptor signaling, which is important in AD pathogenesis, possibly from dysfunctional insulin receptor substrate [4]. There has been interest in developing anti-diabetic pharmacologic mechanisms for AD and dementia therapy [5]. The J20 mouse model is a transgenic animal that overexpresses mutant human amyloid precursor protein (APP) and is widely used as a model for amyloid deposition

and pathogenesis in the study of AD. J20 mice recapitulate many AD-like phenotypes, including synaptic loss, amyloid plaque deposition, and cognitive impairment [6].

Monascus-fermented rice, known as red mold rice (RMR) or red yeast rice (RYR), is a traditional Chinese fermented food used as a color and flavor enhancer. Recent studies indicated that RMR and similar products potentially reverse AD neurodegeneration mainly through the bioactivities of ankaflavin (AK) and monascin (MS). The in vitro studies have proved the neuroprotective effects of RMR against $A\beta_{1–40}$-induced neurotoxicity in PC12 cells [7], while in vivo treatment of rats with RMR improved memory and reduced oxidative stress and inflammation [8]. Our research team previously reported that red mold dioscorea, a red mold fermented product produced from *Dioscorea opposite* root, contained higher levels of MS and AK compared to traditional RMR [9]. MS and AK were previously reported as having numerous clinical effects in non-alcoholic fatty liver, pancreatic disease, and T2DM, as well as anti-oxidant and anti-inflammatory effects [10]. Studies indicated that MS and AK both acted as peroxisome-proliferator-activated receptor (PPAR)-γ agonists, initiating transcription of numerous important downstream metabolic genes [11,12]. PPAR is a ligand-activated type II nuclear receptor highly enriched in adipose tissue. It plays multiple physiological roles in regulations of systemic glucose and lipid metabolism and in the suppression of proinflammatory gene expression, and it is related in AD pathogenesis. Specifically, PPAR-γ agonists might mitigate disease-related pathology and have been found to improve learning and memory in AD animal models [13]. The thiazolidinedione PPAR-γ agonist and rosiglitazone (Ros) were reported to be significantly improved memory and cognition in APP transgenic mice [14].

The aim of the present study was to determine the effects of *Monascus purpureus* fermented product (MPFP), enriched in MS and AK, on the amelioration of cognitive decline and behavioral pathology in the transgenic J20 APP-overexpressing mouse model of AD. The relation to Ros and the underlying mechanisms with relevance to AD therapy are discussed.

2. Materials and Methods

2.1. J20 APP Transgenic Mice

Male heterozygous transgenic mice overexpressing the Swedish ($670/671_{KM\rightarrow NL}$) and Indiana ($717_{V\rightarrow F}$) human APP mutations driven by the platelet-derived growth factor promoter on a C57BL/6J background (line J20) were used, being obtained from Dr. Irene H. Cheng's laboratory (Institute of Brain Science, National Yang-Ming University) (Mucke et al., 2000). The non-AD mouse model C57BL/6 (B6, wild type control) was purchased from BioLASCO Co. (Taipei, Taiwan). The genotype of all transgenic mice was analyzed by PCR analysis on genomic DNA. Mice were housed in a temperature-controlled room (25 °C) on a 12 h light/dark cycle (lights on at 09.00) with ad libitum access to food and water. The 60-day treatment period commenced at age 4 months old, and the mice were euthanized at the end of treatments, when cognitive deficits and Aβ plaques are apparent [15]. All animals received humane care in accordance with the guidelines of the Institutional Animal Care and Use Committee (IACUC) of the National Taiwan Ocean University (IACUC Approval No. 109029).

2.2. In Vivo Drug Treatments

Dose was calculated according to Boyd's formula, as recommended by the U.S. Food and Drug Administration [16]. For a 170 cm tall adult weighing 65 kg, the recommended daily dietary dose of *Monascus purpureus* fermented product (MPFP) is 900 mg, containing 6.0 mg of MS and 2.7 mg of AK. In this study, 30 APP transgenic mice were used who received humane care according to guidelines approved by the Institutional Animal Care and Use Committee of National Taiwan Ocean University (Taiwan, ROC). The C57BL/6J mice were randomly assigned to one of five groups. One group (WT group) consisted of wild-type (WT) mice fed a normal diet (Purina Lab Rodent Diet 5001) and physiological saline. The other groups were as follows: APP transgenic mice (J20 group; fed a normal

diet and physiological saline); onefold dose of MPFP (A1x group; fed a normal diet and 13.50 mg/day/kg of body weight (bw), which included 0.09 mg monascin and 0.042 mg ankaflavin); fivefold dose of MPFP (A5x group; fed a normal diet and 67.50 mg/day/kg bw, which included 0.45 mg monascin and 0.21 mg ankaflavin); and a group treated with rosiglitazone (Ros group; fed a normal diet and 5 mg/day/kg bw). Body weights of the mice were determined weekly.

2.3. Morris Water Maze Test

To assess memory and learning abilities of mice, the Morris water maze (MWM) test was performed. Mice were placed in a water-filled circular pool of 1.1 m diameter with four quadrants each marked by geometric patterns. Poor water temperature was set at 25 °C. Tests were conducted in three parts: pre-training, hidden platform test, and probe test. On the first pre-training day, the platform was set 0.5 cm above the water surface, and mice were allowed 90 s to search for the platform. Those unable to locate the platform in time were gently guided and allowed to rest on it for 1 min. In the hidden platform test conducted between day 2 and 5, the platform was submerged 1 cm below the water surface, and mice were randomly positioned at one of four starting points during each daily session and allowed 90 s to locate the platform. Mice unable to locate the platform were again gently guided. Next, each mouse underwent 4 trials. In the probe test, performed on day 6, the platform was removed, and using a video camera mounted on the ceiling directly above the pool, randomly placed mice were assessed for swimming tracks and latency times to the 4 quadrants. All trials were recorded and analyzed using EthoVision software (Wageningen, The Netherlands).

2.4. Passive Avoidance Test

The passive avoidance test consisted of a shuttle box with light and dark compartments separated by a sliding door. The bottom of the dark compartment consisted of metal rods connected to an electrical current delivery device (constant current shocker model 58006, Lafayette Instruments, Lafayette, IN, USA). Pre-training, shock training, and memory testing were performed on the mice. On pre-training, day 1, mice placed in the light compartment were encouraged to enter the dark compartment when the sliding door was opened. The sliding door was closed for 20 s if they failed to do so spontaneously within 1 min. This was repeated 3 times for each mouse. On day 2, shock training was performed, where mice placed in the light compartment were again encouraged to enter the dark compartment through a sliding door. Within 5 min of entering the dark compartment, a brief electric shock was delivered (100 V, 0.5 mA, 2 s). The mice entered the dark room and were given an electric shock every three seconds. Additional electric shocks were delivered until the mice left the dark compartment, and the number of shocks was recorded. On days 3–5, during the memory test, mice were placed in the light compartment with the sliding door open, and the retention time (maximum of 5 min) in the light compartment was recorded as an index of memory function.

2.5. Measurement of Aβ Levels

In behavioral studies, the mice were euthanized and then brain tissues were recovered. Hippocampi were dissected on ice according to the method of Morawietz et al. (Morawietz et al., 2004), and the tissues were stored at −80 °C until use. Hippocampi were homogenized in 800 mL of 20 mM phosphate-buffered saline (PBS) containing complete protease inhibitor cocktail (Roche, Basel, Switzerland), 0.1 mM sodium orthovanadate (Na_3VO_4), and 1 mM sodium fluoride (NaF). The homogenates were centrifuged at 100,000× *g* for 30 min, and supernatants were used for biochemical assays. Aβ levels were determined by enzyme-linked immunosorbent assay (ELISA), using $A\beta_{1–40}$ and $A\beta_{1–42}$ assay kits according to the manufacturer's protocol (Immuno-Biological Laboratories Co., Ltd., Gunma, Japan), and results are expressed as nmol/g of supernatant protein.

2.6. Measurement of Phosphorylated Tau, TNF-α, and Acetylcholinesterase Activity

Phosphorylated tau (p-tau) levels were determined by a mice phosphorylated microtubule-associated protein tau (pMAPT/pTAU) ELISA kit according to the manufacturer's protocol (Shanghai, China). TNF-α levels were also determined by a mouse TNF-α instant ELISA kit according to the manufacturer's protocol (eBioscience, San Diego, CA, USA). Acetylcholinesterase (AchE) enzyme activity was determined by a QuantiChrom^{TM} AchE assay kit according to the manufacturer's protocol (BioAssay Systems, Hayward, CA, USA).

2.7. Gene Expression Analysis by Quantitative Polymerase Chain Reaction

Total RNA was extracted from hippocampal tissue using the miTotal^{TM} RNA extraction miniprep system following the manufacturer's instructions (Viogene, Sunnyvale, CA, USA). Total RNA was subsequently reverse-transcribed into cDNA, using a high-capacity cDNA reverse transcription kit (Applied Biosystems, Waltham, MA, USA). The samples were processed simultaneously with β-actin as internal control. Data were analyzed using the comparative threshold cycle (ΔΔCt) method. The following primer sequences were used for quantitative polymerase chain reaction (qPCR):

β-actin, forward 5′-CCTGACAGACTACCTCATGAAG-3′, and reverse 5′-CCATCTCTTGCTCGAAGTCTAG-3′; CD36, forward 5′-GAACCACTGCTTTCAAAAACTGG-3′, and reverse 5′-TGCTGTTCTTTGCCACGTCA-3′; BACE1, forward 5′-CCGGCGGGAGTGGTATTATGAAGT-3′, and reverse 5′-GATGGTGATGCGGAAGGACTGATT-3′.

2.8. Immunohistochemistry

2.8.1. Aβ Immunohistochemical Staining

Brain tissue was fixed in 10% formalin at pH 7.4, alcohol-dehydrated, and paraffin-embedded. Serial 35 μm thick sections were cut using a sledge microtome and collected sequentially into culture plate wells in an uninterrupted manner. Sections from regions containing the hippocampus were processed for Aβ immunohistochemical (IHC) staining. Tissue sections were dried at 56 °C for 12 h, deparaffinized, and hydrated. The sections were then sequentially dipped in xylene, gradient concentrations of ethanol, and PBS and treated with 3% hydrogen peroxide for 10 min, followed by several washes PBS at room temperature. The dewax process used 1.7% dishwasher soap aqueous solution at 90 °C, which was applied before staining, and this was followed oven drying that was conducted before cover slipping to eliminate xylene from the staining tasks. Then, the avidin–biotin complex method was applied for labeling. The sections were treated with 10% normal horse serum in PBS for the blocking process, and then were placed in primary monoclonal 6E10 anti-β amyloid antibody for 60 min. After washing with PBS, the sections were incubated with the polyvalent biotinylated antibody agent (1:500) for 45 min and washed again with PBS. Antibody labeling was detected using diaminobenzidine (DAB) peroxidase substrate.

2.8.2. APP IHC Stain

Up to half of the brains each was sampled and fixed in formalin (10%) for 24 h. After washing and dehydration, the portion containing the hippocampus was embedded in paraffin. The tissues were sliced and collected on glass slides and then dried and deparaffinized (Bancroft and Gamble, 2008). Sections were covered with 3% H_2O_2 in methanol for 10 min to quench endogenous peroxidase activity and then blocked with 5% bovine serum albumin protein in Tris-buffered saline. After blocking, sections were sequentially treated with primary antibody (polyclonal rabbit anti-β amyloid precursor antibody, LS-B1462, LSBio, Seattle, WA, USA), biotinylated anti-rabbit secondary antibody, and avidin-labelled peroxidase, and then diaminobenzidine was added for visualization.

2.9. Statistical Analysis

Data are expressed as the mean ± standard deviation (SD). The statistical significance of the biochemical analysis was determined by one-way analysis of variance (ANOVA), and Duncan's multiple range test was used to compare differences between groups' model

procedure through Statistical Product and Service Solutions software (SPSS Institute, Inc., Chicago, IL, USA). Possibility of $p < 0.05$ was applied and considered as a statistically significant difference.

3. Results

3.1. MPFP Significantly Improved Cognitive Behavior, Learning, and Memory Ability

The determination of MPFP on the effects of reversed cognitive behavioral abnormalities and improved learning and memory ability were conducted using 4-month-old J20 mice. A standard diet fortified with 1× or 5× MPFP or administered rosiglitazone was provided for 8 weeks. WT littermates were fed as the standard diet during the experimental period. There were no significant differences found in the body weights of mice between groups over the treatment courses (data not shown).

The behavior, learning, and memory schedule of the animal experiment occurred during weeks 7–8. Passive or active avoidance fear conditioning with MWM is often used in animal behavioral testing, in which animals rely on different motor and sensory abilities; these tests can be performed reliably on the same animal [17]. The passive avoidance test was applied in this study to evaluate the development of fear memory in mice. During the shock training, untreated J20 mice received significantly more shocks than the WT mice, indicating that J20 mice had impaired fear memory. Figure 1a shows the number of times that each group was subjected to electrodes during the second day of electric shock training. It can be found that the average number of electric shocks in the J20 group was about six times, which is significantly higher than that in the wild-type control group. It is inferred that the J20 mouse has a difficult memory formation in terms of avoiding the dark room. Conversely, mice in the A1x, A5x, and Ros groups displayed significantly lower numbers of shocks than those in the J20 group, with performance comparable to WT animals (Figure 1a). Thus, A1x, A5x, and Ros treatment in the setting of APP overexpression appeared to restore normal fear memory development compared with untreated J20 mice. As shown in Figure 1b, 3-day consecutive memory trials following shock training showed significantly reduced light compartment latency times for untreated J20 mice compared with WT mice, especially over repeated attempts. This indicates that MPFP slightly improved learning and memory in the J20 AD mice.

Moreover, spatial learning and memory, as evaluated by MWM, was significantly improved in the A1x, A5x, and Ros treatment groups compared with untreated J20 mice, and approaching performance of WT mice (Figure 1c). Pre-training, performed on day 1, revealed no significant differences in visual or motor memory performance among the groups. On the hidden platform test (days 2–5), untreated J20 mice required a considerably longer duration locating the platform than WT mice, and their search time did not measurably decrease over four consecutive training days, consistent with impaired spatial learning and memory. The A1x, A5x, and Ros groups, however, were significantly faster at locating the platform and had progressively decreasing search times across the training period compared with untreated J20 mice, indicating improved learning and memory.

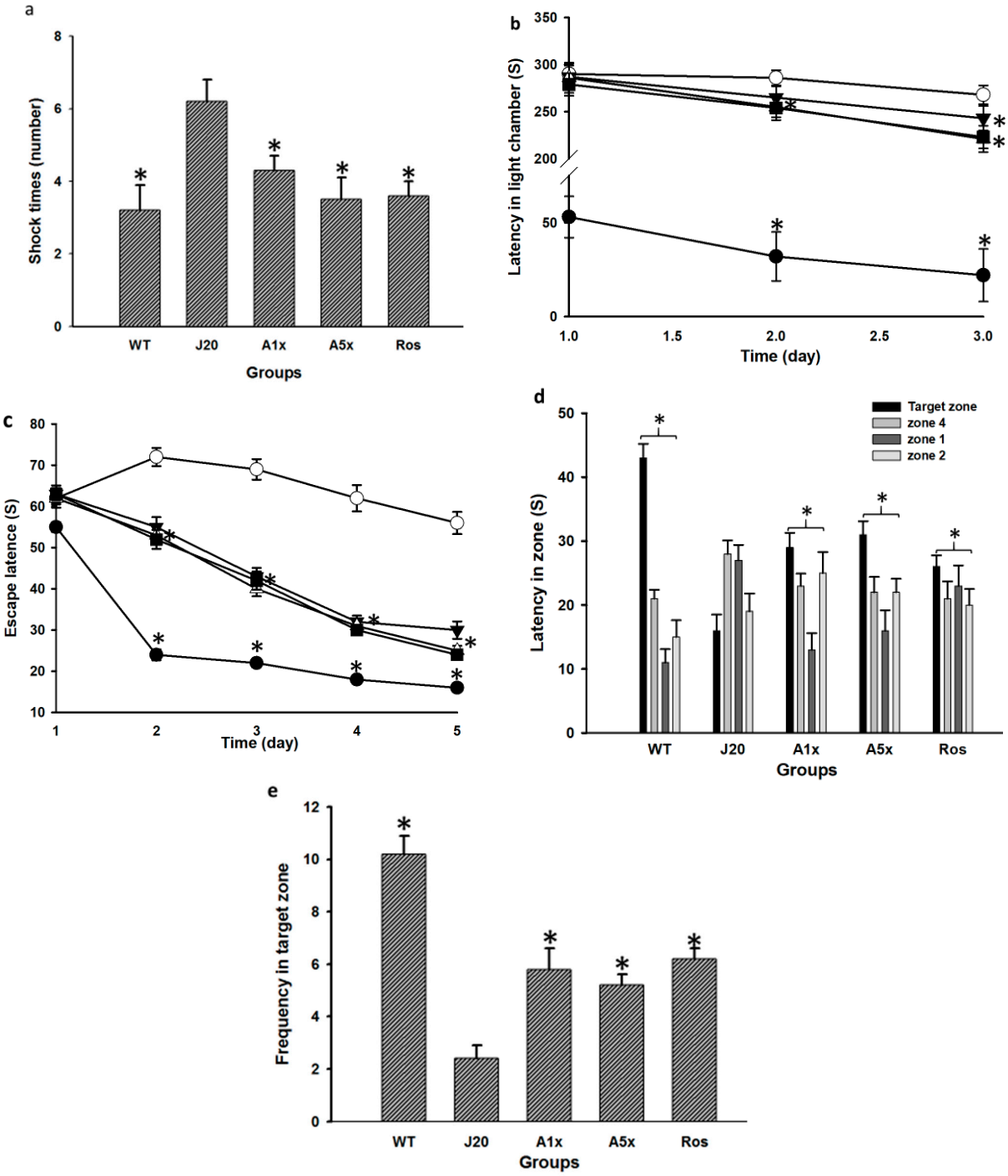

Figure 1. Effects of MPFP on memory and learning in J20 mice. (**a**) Electric shock training for the passive avoidance task. (**b**) Latency time to the light chamber. (**c**) Water maze test search for the hidden platform. (**d**) Latency and (**e**) frequency to the target zone for mice in the probe test. The C57BL/6J mice were randomly assigned to one of five groups. One group (WT group) consisted of wild-type (WT) mice fed a normal diet (Purina Lab Rodent Diet 5001) and physiological saline (WT group, ●). The other groups were as follows: APP transgenic mice (J20 group; fed a normal diet and physiological saline, ○), onefold dose of MPFP (A1x group; fed a normal diet and 13.50 mg/day/kg of body weight (bw), which included 0.09 mg monascin and 0.042 mg ankaflavin, ▼), fivefold dose of MPFP (A5x group; fed a normal diet and 67.50 mg/day/kg bw, which included 0.45 mg monascin and 0.21 mg ankaflavin, △), and a group treated with rosiglitazone (Ros group; fed a normal diet and 5 mg/day/kg bw, ■). Each value is expressed as a mean ± SD (n = 6). * $p < 0.05$ versus J20 group.

As an index of memory function, a 90 s spatial probe trial was also conducted on day 6 of the MWM with the platform removed to assess duration time in the target zone platform. As shown in Figure 1d, memory-impaired J20 mice spent markedly less time in the target zone than WT mice, but the Ros, A1x, and A5x groups all showed significantly increased retention time in the target zone compared with J20 mice, suggesting that the treatments ameliorated spatial memory dysfunction. Although latency time to the target zone is a useful indicator of spatial memory, it may not be as reliable under certain conditions, such as when mice linger at the target zone boundary line. Therefore, the frequency of entering into the target zone as a confirmatory index of spatial memory retention was measured as well. As illustrated in Figure 1e, A1x and A5x mice, along with WT and Ros groups, had significantly higher target zone entry frequencies than those in the J20 group, further confirming spatial memory improvement in the treated and J20 groups. Additionally, to visually confirm spatial memory improvement, swimming tracks of the mice were recorded. Mice in the untreated J20 group clearly displayed directionless and random search patterns almost encompassing the entire pool, whereas the search patterns of the A1x, A5x, and WT were focused primarily on the target zone (Figure S1). Collectively, similar to treatment with Ros, treatment of J20 APP transgenic mice with MPFP significantly improved learning and memory when compared with untreated J20 mice.

3.2. MPFP Treatment Reduced Brain Aβ Levels

To determine the impact of MPFP on brain amyloid production, hippocampal Aβ levels in J20 transgenic mice were determined by ELISA after 60 day of treatment. Mice in the A1x, A5x, and Ros groups all showed significantly lower hippocampal $A\beta_{1–40}$ levels compared with untreated J20 mice (Figure 2a). The treatment of MPFP at either dose appeared as effective as Ros treatment in lowering $A\beta_{1–40}$. Moreover, hippocampal $A\beta_{1–42}$ levels were also significantly reduced (Figure 2b) in treated mice compared with untreated J20 transgenic mice. For $A\beta_{1–40}$ and $A\beta_{1–42}$, a dose response reduction in Aβ levels was observed with increasing doses of MPFP.

In the neuropathology observation, J20 mice exhibited hippocampal APP expression, while no Aβ plaques were found in 1× or 5× MPFP-treated, Ros-treated, or WT animals (Figure 2c,d), suggesting that 1× or 5× MPFP might suppress hippocampal amyloid plaque formation. MPFP appeared to rescue memory impairment in J20 mice in association with reduced hippocampal amyloid burden.

3.3. MPFP Enhanced Brain Cholinergic Activity in J20 Mice

Basal forebrain cholinergic deficit is a consistent feature in AD [18] that is targeted by AChE inhibitor therapy [19]. The brain cholinergic activity was determined by measuring AChE activity. AChE activity was low in WT mice, while untreated J20 mice showed high activity. The hippocampal AChE activities were high in all treated and untreated J20 transgenic mice compared to WT. However, the administration of 1× or 5× MPFP or Ros to J20 mice showed significantly inhibited AChE activity (Figure 3a) compared to untreated J20. MPFP treatment was found the possibility of partially restore cholinergic function.

3.4. Effect of MPFP on TNF-α and Neuroinflammation

Upregulation of the pro-inflammatory cytokine TNF-α resulted the acceleration of AD pathogenesis and the cognitive decline in AD [20]. Hippocampal TNF-α levels were found markedly higher in J20 mice than in WT, suggesting that amyloid overexpression is associated with a pro-inflammatory state (Figure 3b). Treatment with 1× or 5× MPFP or Ros significantly decreased TNF-α levels, as well hippocampal levels, perhaps caused by whole-brain neuroinflammation in the J20 mouse model.

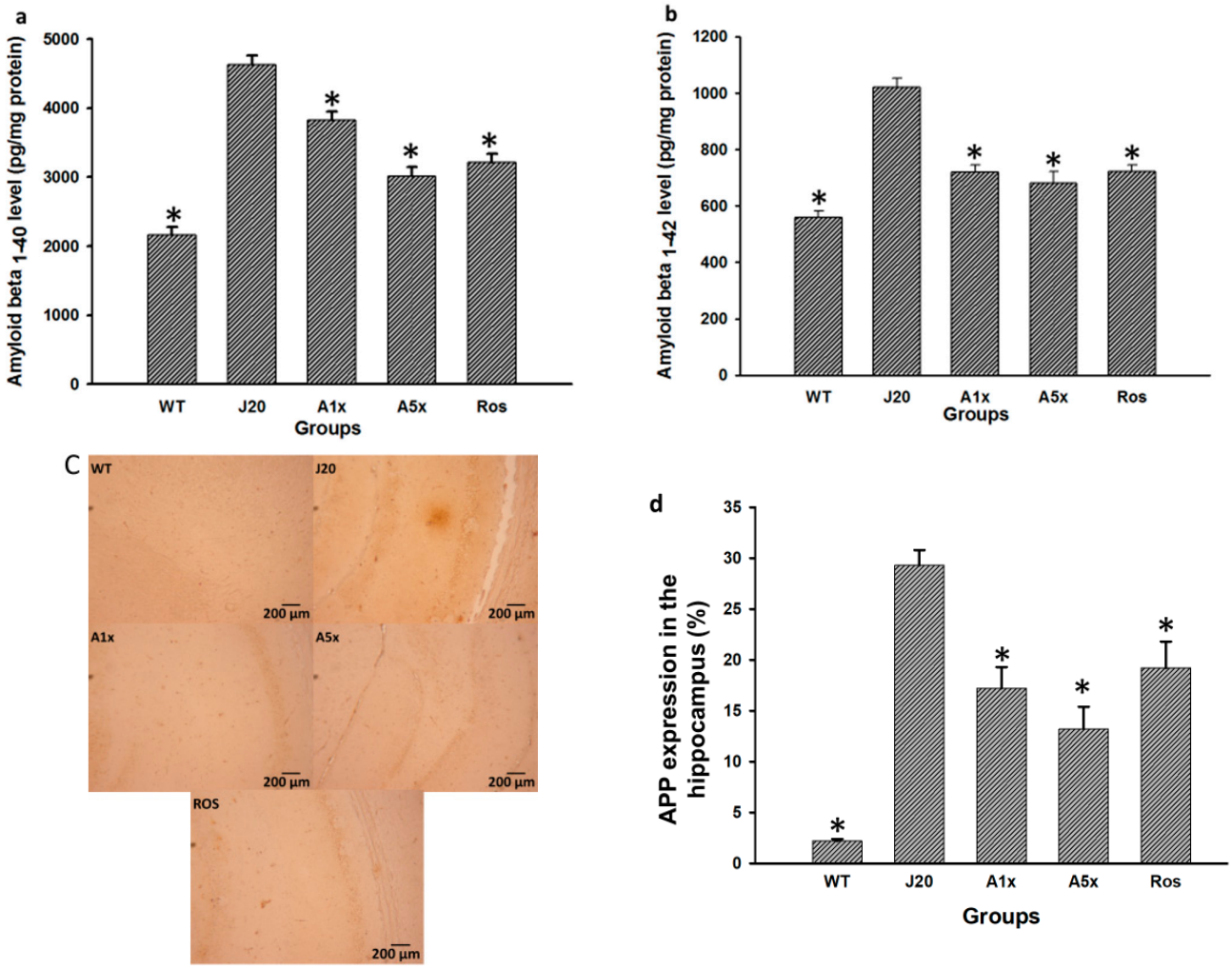

Figure 2. Effects of MPFP on Aβ expression in the hippocampus of J20 mice. (**a**) $A\beta_{1–40}$ levels; (**b**) $A\beta_{1–42}$ levels; (**c**) APP histologicexpression was examined using immunohistochemical staining (brown); (**d**) Hippocampal APP expression levels in each group. Abbreviations for each group are as in Figure 1. Each value is expressed as a mean ± SD (n = 6). * $p < 0.05$ versus J20 group.

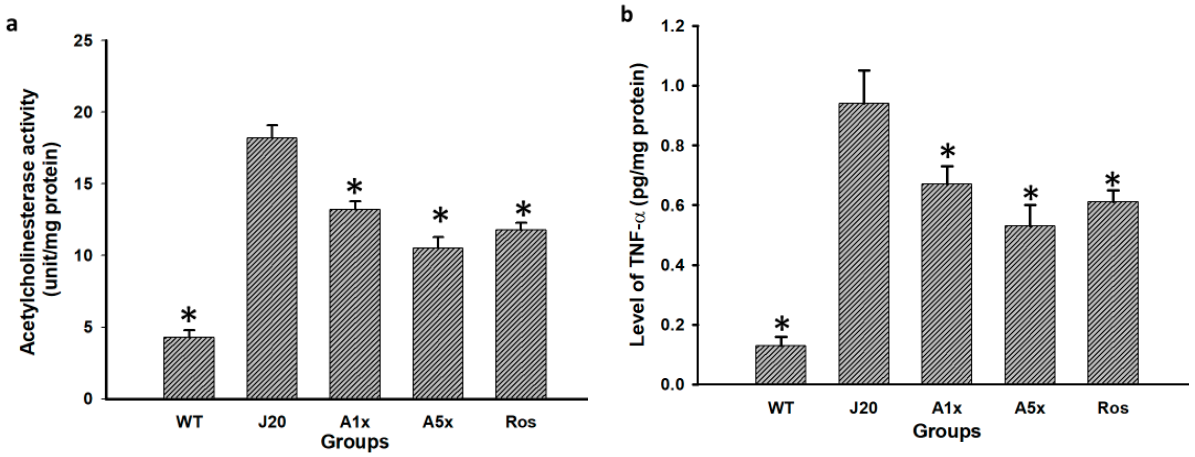

Figure 3. Effects of MPFP on AD-related factors in the hippocampus of J20 mice. (**a**) Acetylcholinesterase; (**b**) TNF-α level. Abbreviations for each group are as in Figure 1. Each value is expressed as the mean ± SD (n = 6). * $p < 0.05$ versus J20 group.

3.5. MPFP Improved AD-Related Gene Expression

The investigation for the effect of MPFP on AD-related genes in J20 transgenic mice was designed by examining the brain expression of several AD-relevant genes, including BACE1, APP, and CD36. The treatments of MPFP and Ros were compared to untreated J20 and WT mice. BACE1 is considered an important factor for the amyloid genic processing of APP and currently is being used as a target for the development of AD therapies. As illustrated in Figure S2a, hippocampal BACE1 gene expression in J20 mice treated with 1× or 5× MPFP or Ros versus untreated J20 and WT mice were compared. Similar to Ros treatment, A1x and A5x treatments significantly reduced BACE1 gene expression. Furthermore, the effects of MPFP treatment on the APP gene expression in the hippocampus were tested. The results showed IHC against APP demonstrated considerably higher hippocampal APP immunoreactivity in J20 mice than in the WT group, which is consistent with APP overexpression in J20 mice. Interestingly, APP immunoreactivity was higher in the 1× and 5× MPFP-treated groups than in untreated J20 mice (Figure S2b), indicating that MPFP treatment augmented APP expression. It is possible that in this model, MPFP-induced reduction of BACE1 expression leads to reduced APP proteolysis, increased intact APP, and less Aβ.

In order to elucidate the effect of MPFP on the Aβ-associated neuroinflammatory response, the gene expression of CD36 scavenger receptor, an index of Aβ-related microglial activation [21], was measured. Treatments with both MPFP and Ros significantly increased hippocampal CD36 gene expression in J20 mice (Figure S2c). Moreover, A1x and A5x treatments increased CD36 expression in a dose-dependent manner. Taken together, despite of elevating APP expression, MPFP downregulated brain Aβ production not only occurred by inhibiting BACE1 expression but also by activating CD36-positivemicroglia to facilitate the clearance of brain Aβ.

4. Discussion

In this study, MPFP effects on AD was demonstrated, which significantly improved learning and memory in the J20 transgenic mouse model of AD. Previously, our group showed that RMR effectively ameliorated AD symptoms by suppressing Aβ 40 accumulation, oxidative stress, and the inflammatory response [7]. Several functional factors contained in RMR, such as azaphilone pigments (anti-inflammatory), γ-aminobutyric acid (neurotransmitter), and lovastatin (anti-lipid agent), were reported as effective matters against AD pathology in animal models. Another active chemical called statins in RMR were previously shown to have a very high effect on the reduction of Aβ in a transgenic AD mouse model [22].

Monascus species produce several functional bioactive pigments, including the yellow pigments (AK and MS), orange pigments (monascorubrin and rubropunctanin), and red pigments (monascorubramine and rubropuctamine), of which AK and MS are the major components [23]. In this study, there is no purified MS and AK used, and only the fermented product MPFP was tested. This remains a goal for future investigation. Nonetheless, in previous studies, MS and AK were found to act as PPAR-γ agonists [11,12], and numerous studies have demonstrated the efficacy of PPAR-γ agonists in ameliorating disease-related pathology and improving learning and memory in AD animal models [24]. Consistent with this, Ros also improved cognition and spatial memory in AD mice by reducing Aβ and tau pathology [25]. While it remains unknown as to how exactly PPAR-γ ameliorates AD pathology, PPAR-γ (and presumably MPFP/MS and AK) probably acts through multiple mechanisms [13].

As PPAR-γ activation may be critical to MPFP/MS and AK bioactivity, Ros was included in our study, which is a high-affinity thiazolidinedione PPAR-γ agonist for comparison. Ros is widely used in diabetic therapy, markedly improving insulin sensitivity through activation of PPAR-γ and retinoic X receptor (RXR) and downstream modulation of PPAR response element (PPRE) binding to gene promoter regions to alter gene transcription. Given the overlap between metabolic disease and neurodegeneration, Ros has

been a therapeutic target of interest in AD. In APP transgenic mice, Ros has been shown to improve behavioral performance, activate Wnt signaling, normalize brain glucocorticoid receptor levels, and decrease insoluble Aβ42 levels [25–27]. Furthermore, insulin receptor substrate-1/2 in the insulin signaling pathway has been implicated as an important pathogenic step in AD; Ros could potentially replenish brainIRS-1/2 function, which could be beneficial in this regard. MPFP (AK and MS) may act in parallel to Ros in these respects.

Moreover, MPFP might alter amyloid processing through PPAR-γ signaling [28]. PPAR-γ activation might cause binding to the PPRE in the upstream region of the BACE1 gene promoter, thereby suppressing BACE1 activity. Furthermore, our compound might exert a neuroprotective effect through a concomitantly increase secreted APPα (sAPPα) production. Neurotrophic and neuroprotective sAPPα is naturally produced via an alternative APP cleavage pathway that precludes Aβ production [29]. Our research team previously showed that RMR increases levels of sAPPα, reduces Aβ40, prevents neurodegeneration, and improves cognition in rats [30]. As MPFP (MS, AK) is very similar to RMR, it is likely that it also promotes sAPPα production, which will be investigated in the future.

Other mechanisms by which MPFP might ameliorate neurodegeneration in AD include a reduction of tau aggregation and modulation of neuroinflammation. Tau dysfunction in AD brains leads to aberrant formation of aggregated forms such as paired helical filaments and NFTs, which likely interfere with axonal transport. Indeed, in our study, both Ros and MPFP significantly reduced hippocampal tau phosphorylation. PPAR-γ could potentially reduce pTau through modified Wnt signaling, reduced GSK3β activity, and increased β-catenin [31]. Furthermore, PPAR-γ activation has been shown to reduce tau phosphorylation in vitro via a non-Akt-dependent pathway through nuclear translocation of phosphoinositide-dependent protein kinase 1 (PDK1) and reducing cytosolic phosphorylated 70 kDa ribosomal protein kinase (p70S6) and phosphorylated mammalian target of rapamycin (mTor) [32]. Alternatively, both Ros and the thiazolidinedione troglitazone decreased CDK5-induced tau phosphorylation through proteosomal degradation of p35 [33]

Mediated by various cytokines, neuroinflammation in the AD brain triggers microglial activation in response to aggregated Aβ to facilitate phagocytic Aβ clearance [34]. Previously, PPAR-γ agonists showed increased phagocytic clearance of amyloid by activating microglia [35]. Our finding proved that Ros and MPFP both upregulate hippocampal CD36, which was expressed on the microglial surface in relation to Aβ phagocytosis, in a dose-dependent manner in J20 mice, suggesting that PPAR-γ activation might underlie beneficial neuroinflammatory mechanisms enhancing Aβ clearance. In addition, our compound also reduced the secretion of harmful pro-inflammatory cytokines such as TNF-α, which was previously shown to inhibit Aβ clearance in AD [36]. Therefore, further research is required to elucidate the effect mechanisms of beneficial and detrimental neuroinflammatory activation.

5. Conclusions

As the prevailing framework for AD pathogenesis, amyloid hypothesis predicts that a reduction in brain Aβ production by inhibiting BACE1 or γ-secretase activity, or a decrease in Aβ deposition and toxicity through immunotherapy or other strategies, can prevent disease progression and improve cognitive outcomes. Recently, disappointing results of AD clinical therapy trials made it increasingly apparent that such an approach might be of limited efficacy. Briefly, preventing Aβ production or deposition alone might be important but not sufficient to prevent neurodegeneration and cognitive decline. MPFP along with MS and AK represent promising therapeutic candidates for AD. They were tested in the study, likely via many evaluations such as PPAR-γ-dependent mechanisms, reversed cognitive decline, and behavioral deficits in J20 APP transgenic mice. Among the various possible downstream actions of PPAR-γ, including anti-diabetic effects, inhibition of BACE1-mediated Aβ production, reduction of aberrant tau phosphorylation, and modulation of neuroinflammation, perhaps the most intriguing possibility is that MPFP might

shift APP processing from amyloidogenic to pro-neurotrophic sAPPα. Often overlooked as a factor in AD, sAPPα is essential for normal neurosynaptic activity, and may be a missing component to a more complete and efficacious disease-modifying therapy for AD [29]. In use as a traditional dietary supplement, MPFP appears safe in humans, but further work is required to address questions regarding the mechanism of action and to establish its precise clinical safety and efficacy in AD patients (Figure S3).

Supplementary Materials: The following supporting information can be downloaded at https://www.mdpi.com/article/10.3390/fermentation8050193/s1. Figure S1. Effects of MPFP on the swimming tracks of J20 mice in the water maze probe test. Figure S2. Effects of MPFP on AD pathology in the hippocampus of J20 mice. Figure S3. The red lines indicate the possible mechanism of Monascus purpureus fermented product ameliorating Alzheimer's disease.

Author Contributions: M.-C.F., I.H.-J.C. and C.-L.C. drafted the paper. M.-C.F., I.H.-J.C. and C.-L.C. performed the experiments. All authors have read and agreed to the published version of the manuscript.

Funding: This research did not receive any specific grant from funding agencies in the public, commercial, or not-for-profit sectors.

Institutional Review Board Statement: All animals received humane care in accordance with the guidelines of the Institutional Animal Care and Use Committee (IACUC) of the National Taiwan Ocean University (IACUC Approval No. 109029).

Informed Consent Statement: Not applicable.

Data Availability Statement: All authors will share their original data freely.

Conflicts of Interest: All authors have no conflict of interest to declare.

References

1. Querfurth, H.W.; LaFerla, F.M. Alzheimer's disease. *N. Engl. J. Med.* **2010**, *362*, 329–344. [CrossRef] [PubMed]
2. Mattson, M.P. Pathways towards and away from Alzheimer's disease. *Nature* **2004**, *430*, 631–639. [CrossRef] [PubMed]
3. Di Filippo, M.; Sarchielli, P.; Picconi, B.; Calabresi, P. Neuroinflammation and synaptic plasticity: Theoretical basis for a novel, immune-centred, therapeutic approach to neurological disorders. *Trends Pharmacol. Sci.* **2008**, *29*, 402–412. [CrossRef] [PubMed]
4. Kleinridders, A.; Ferris, H.A.; Cai, W.; Kahn, C.R. Insulin action in brain regulates systemic metabolism and brain function. *Diabetes* **2014**, *63*, 2232–2243. [CrossRef]
5. Sims-Robinson, C.; Kim, B.; Rosko, A.; Feldman, E.L. How does diabetes accelerate Alzheimer disease pathology? *Nat. Rev. Neurol.* **2010**, *6*, 551–559. [CrossRef]
6. Tosh, J.L.; Rickman, M.; Rhymes, E.; Norona, F.E.; Clayton, E.; Mucke, L.; Isaacs, A.M.; Elizabeth, M.C.; Fisher, E.C.M.; Wiseman, F.K. The integration site of the APP transgene in the J20 mouse model of Alzheimer's disease. *Wellcome Open Res.* **2018**, *2*, 84. [CrossRef]
7. Lee, C.L.; Wang, J.J.; Pan, T.M. Red mold rice extract represses amyloid beta peptide-induced neurotoxicity via potent synergism of anti-inflammatory and antioxidative effect. *Appl. Microbiol. Biotechnol.* **2008**, *79*, 829–841. [CrossRef]
8. Lee, C.L.; Kuo, T.F.; Wang, J.J.; Pan, T.M. Red mold rice ameliorates impairment of memory and learning ability in intracerebroventricular amyloid beta-infused rat by repressing amyloid beta accumulation. *J. Neurosci. Res.* **2007**, *85*, 3171–3182. [CrossRef]
9. Lee, C.L.; Wang, J.J.; Kuo, S.L.; Pan, T.M. *Monascus* fermentation of dioscorea for increasing the production of cholesterol-lowering agent—Monacolin K and antiinflammation agent—Monascin. *Appl. Microbiol. Biotechnol.* **2006**, *72*, 1254–1262. [CrossRef]
10. Lee, B.H.; Hsu, W.H.; Huang, T.; Chang, Y.Y.; Hsu, Y.W.; Pan, T.M. Monascin improves diabetes and dyslipidemia by regulating PPARgamma and inhibiting lipogenesis in fructose-rich diet-induced C57BL/6 mice. *Food Funct.* **2013**, *4*, 950–959. [CrossRef]
11. Hsu, W.H.; Lee, B.H.; Chang, Y.Y.; Hsu, Y.W.; Pan, T.M. A novel natural Nrf2 activator with PPARγ-agonist (monascin) attenuates the toxicity of methylglyoxal and hyperglycemia. *Toxicol. Appl. Pharmacol.* **2013**, *272*, 842–851. [PubMed]
12. Hsu, W.H.; Lee, B.H.; Liao, T.H.; Hsu, Y.W.; Pan, T.M. *Monascus*-fermented metabolite monascin suppresses inflammation via PPAR-gamma regulation and JNK inactivation in THP-1 monocytes. *Food Chem. Toxicol.* **2012**, *50*, 1178–1186. [CrossRef] [PubMed]
13. Landreth, G.; Jiang, Q.; Mandrekar, S.; Heneka, M. PPAR gamma agonists as therapeutics for the treatment of Alzheimer's disease. *Neurotherapeutics* **2008**, *5*, 481–489. [CrossRef] [PubMed]
14. Escribano, L.; Simon, A.M.; Gimeno, E.; Cuadrado-Tejedor, M.; Lopez de Maturana, R.; Garcia-Osta, A.; Ricobaraza, A.; Perez-Mediavilla, A.; Del Rio, J.; Frechilla, D. Rosiglitazone rescues memory impairment in Alzheimer's transgenic mice: Mechanisms involving a reduced amyloid and tau pathology. *Neuropsychopharmacology* **2010**, *35*, 1593–1604. [CrossRef] [PubMed]

15. Cheng, I.H.; Scearce-Levie, K.; Legleiter, J.; Palop, J.J.; Gerstein, H.; Bien-Ly, N.; Puolivali, J.; Lesne, S.; Ashe, K.H.; Muchowski, P.J.; et al. Accelerating amyloid-beta fibrillization reduces oligomer levels and functional deficits in Alzheimer disease mouse models. *J. Biol. Chem.* **2007**, *282*, 23818–23828. [CrossRef]
16. Ratner, M. FDA pharmacogenomics guidance sends clear message to industry. *Nat. Rev. Drug Discov.* **2005**, *4*, 359. [CrossRef]
17. Crawley, J.N. *What's Wrong with My Mouse? Behavioral Phyenotyping of Transgenic and Knockout Mice*, 2nd ed.; Wiley-Interscience: Hoboken, NJ, USA, 2007.
18. Arendt, T.; Bigl, V.; Tennstedt, A.; Arendt, A. Correlation between cortical plaque count and neuronal loss in the nucleus basalis in Alzheimer's disease. *Neurosci. Lett.* **1984**, *48*, 81–85.
19. Aucoin, J.S.; Jiang, P.; Aznavour, N.; Tong, X.K.; Buttini, M.; Descarries, L.; Hamel, E. Selective cholinergic denervation, independent from oxidative stress, in a mouse model of Alzheimer's disease. *Neuroscience* **2005**, *132*, 73–86.
20. Holmes, C.; Cunningham, C.; Zotova, E.; Woolford, J.; Dean, C.; Kerr, S.; Culliford, D.; Perry, V.H. Systemic inflammation and disease progression in Alzheimer disease. *Neurology* **2009**, *73*, 768–774. [CrossRef]
21. Richter, B.; Bandeira-Echtler, E.; Bergerhoff, K.; Clar, C.; Ebrahim, S.H. Rosiglitazone for type 2 diabetes mellitus. *Cochrane Database Syst. Rev.* **2007**, *18*, CD006063.
22. Scott, H.D.; Laake, K. Statins for the prevention of Alzheimer's disease. *Cochrane Database Syst. Rev.* **2001**, *3*, CD003160.
23. Shi, Y.C.; Pan, T.M. Beneficial effects of *Monascus purpureus* NTU 568-fermented products: A review. *Appl. Microbiol. Biotechnol.* **2011**, *90*, 1207–1217. [CrossRef] [PubMed]
24. Heneka, M.T.; Sastre, M.; Dumitrescu-Ozimek, L.; Hanke, A.; Dewachter, I.; Kuiperi, C.; O'Banion, K.; Klockgether, T.; Van Leuven, F.; Landreth, G.E. Acute treatment with the PPARγ agonist pioglitazone and ibuprofen reduces glial inflammation and Aβ1–42 levels in APPV717I transgenic mice. *Brain* **2005**, *128*, 1442–1453. [CrossRef] [PubMed]
25. Escribano, L.; Simon, A.M.; Perez-Mediavilla, A.; Salazar-Colocho, P.; Del Rio, J.; Frechilla, D. Rosiglitazone reverses memory decline and hippocampal glucocorticoid receptor down-regulation in an Alzheimer's disease mouse model. *Biochem. Biophys. Res. Commun.* **2009**, *379*, 406–410. [CrossRef] [PubMed]
26. Pedersen, W.A.; McMillan, P.J.; Kulstad, J.J.; Leverenz, J.B.; Craft, S.; Haynatzki, G.R. Rosiglitazone attenuates learning and memory deficits in Tg2576 Alzheimer mice. *Exp. Neurol.* **2006**, *199*, 265–273. [CrossRef]
27. Toledo, E.M.; Inestrosa, N.C. Activation of Wnt signaling by lithium and rosiglitazone reduced spatial memory impairment and neurodegeneration in brains of an APPswe/PSEN1DeltaE9 mouse model of Alzheimer's disease. *Mol. Psychiatry* **2010**, *15*, 272–285. [CrossRef]
28. Sastre, M.; Dewachter, I.; Rossner, S.; Bogdanovic, N.; Rosen, E.; Borghgraef, P.; Evert, B.O.; Dumitrescu-Ozimek, L.; Thal, D.R.; Landreth, G.; et al. Nonsteroidal anti-inflammatory drugs repress beta-secretase gene promoter activity by the activation of PPARγ. *Proc. Natl. Acad. Sci. USA* **2006**, *103*, 443–448. [CrossRef]
29. Habib, A.; Sawmiller, D.; Tan, J. Restoring soluble amyloid precursor protein α functions as a potential treatment for Alzheimer's disease. *J. Neurosci. Res.* **2017**, *95*, 973–991. [CrossRef]
30. Lee, C.L.; Kuo, T.F.; Wu, C.L.; Wang, J.J.; Pan, T.M. Red mold rice promotes neuroprotective sAPPα secretion instead of Alzheimer's risk factors and amyloid beta expression in hyperlipidemic Aβ40-infused rats. *J. Agric. Food Chem.* **2010**, *58*, 2230–2238. [CrossRef]
31. Inestrosa, N.C.; Godoy, J.A.; Quintanilla, R.A.; Koenig, C.S.; Bronfman, M. Peroxisome proliferator-activated receptor γ is expressed in hippocampal neurons and its activation prevents β-amyloid neurodegeneration: Role of Wnt signaling. *Exp. Cell Res.* **2005**, *304*, 91–104. [CrossRef]
32. d'Abramo, C.; Ricciarelli, R.; Pronzato, M.A.; Davies, P. Troglitazone, a peroxisome proliferator-activated receptor-gamma agonist, decreases tau phosphorylation in CHOtau4R cells. *J. Neurochem.* **2006**, *98*, 1068–1077. [CrossRef] [PubMed]
33. Cho, D.; Lee, E.J.; Kwon, K.J.; Shin, C.Y.; Song, K.; Park, J.; Jo, I.; Han, S. Troglitazone, a thiazolidinedione, decreases tau phosphorylation through the inhibition of cyclin-dependent kinase 5 activity in SH-SY5Y neuroblastoma cells and primary neurons. *J. Neurochem.* **2013**, *126*, 685–695. [CrossRef] [PubMed]
34. Lee, C.Y.; Landreth, G.E. The role of microglia in amyloid clearance from the AD brain. *J. Neural Transm.* **2010**, *117*, 949–960. [CrossRef] [PubMed]
35. Yamanaka, M.; Ishikawa, T.; Griep, A.; Axt, D.; Kummer, M.P.; Heneka, M.T. PPARγ/RXRα-induced and CD36-mediated microglial amyloid-β phagocytosis results in cognitive improvement in amyloid precursor protein/presenilin mice. *J. Neurosci.* **2012**, *32*, 17321–17331. [CrossRef]
36. Hickman, S.E.; Allison, E.K.; El Khoury, J. Microglial dysfunction and defective beta-amyloid clearance pathways in aging Alzheimer's disease mice. *J. Neurosci.* **2008**, *28*, 8354–8360. [CrossRef]